Journal of Computational Physics 231 (2012) 1879–1899

Contents lists available at SciVerse ScienceDirect

Journal of Computational Physics

journal homepage: www.elsevier.com/locate/jcp

A fast direct solver for the integral equations of scattering theory on planar curves with corners

James Bremer *

Department of Mathematics, University of California, Davis, CA 95616, USA

ARTICLE INFO

Article history:
Received 2 June 2011
Received in revised form 18 October 2011
Accepted 9 November 2011
Available online 22 November 2011

Keywords:
Integral equations
Corner singularities
Elliptic boundary value problems
Scattering theory

ABSTRACT

We describe an approach to the numerical solution of the integral equations of scattering theory on planar curves with corners. It is rather comprehensive in that it applies to a wide variety of boundary value problems; here, we treat the Neumann and Dirichlet problems as well as the boundary value problem arising from acoustic scattering at the interface of two fluids. It achieves high accuracy, is applicable to large-scale problems and, perhaps most importantly, does not require asymptotic estimates for solutions. Instead, the singularities of solutions are resolved numerically. The approach is efficient, however, only in the low- and mid-frequency regimes. Once the scatterer becomes more than several hundred wavelengths in size, the performance of the algorithm of this paper deteriorates significantly. We illustrate our method with several numerical experiments, including the solution of a Neumann problem for the Helmholtz equation given on a domain with nearly 10000 corner points.

0. Introduction

This work is founded on two simple observations. The first is that certain classes of integral operators given on Lipschitz curves are well-conditioned when considered as operators on spaces of square integrable functions. This is a consequence of the resistance of L^2 estimates to pathologies situated on sets of measure zero. The second observation is that the "scattering matrix" formalism of physics provides a mechanism for accelerating the numerical calculations necessary to solve non-oscillatory elliptic boundary value problems. When combined, these ideas yield a comprehensive approach to the solution of the boundary value problems of scattering theory on singular domains, assuming only that the scatterer is relatively small when measured in wavelengths.

We concentrate here on a particularly simple class of elliptic boundary value problems: those associated with the constant coefficient Helmholtz equation given on planar domains with corners points. Problems of this type can be profitably reformulated as boundary integral equations and our method is based on such an approach.

The numerical solution of integral equations given on planar domains with corners has been widely studied, but only a few existing approaches are capable of achieving high accuracy. The article [20] introduced one of the first such methods. However, because this method makes use of a global quadrature rule it requires modification in order to apply it to domains with more than one corner point. Moreover, it relies on analytic estimates applicable only to the Dirichlet problem for Laplace's equation. The contribution [8] is similar in spirit to [20]. It introduces a scheme for the numerical solution of Neumann problems for Laplace's equation given on planar domains with corners. Unlike the Dirichlet problem for Laplace's equation, the solutions of the standard integral equation formulation of the Neumann problem for Laplace's equation can

* Tel.: +1 203 843 4916.
E-mail address: bremer@math.ucdavis.edu

0021-9991/$ - see front matter © 2011 Elsevier Inc. All rights reserved.
doi:10.1016/j.jcp.2011.11.015

exhibit singularities which are unbounded in L^∞ norm. This is addressed in [8] through subtraction of singularities and specialized global quadrature rules. While this approach is able to achieve high-accuracy, it suffers from the same drawbacks as [20]: limited applicability due to the use of extensive analytic knowledge of solutions and global quadrature. The article [1] describes a scheme for solving Neumann problems for the Helmholtz equation given on domains with corners based on a nonstandard integral equation formulation whose solutions do not exhibit unbounded singularities. This is a promising approach, but it is not yet clear if it can be extended to the many boundary integral formulations which arise from electromagnetic and acoustic scattering on surfaces.

The work described in [15–18], which centers on an approach dubbed "compressed inverse preconditioning," is quite generally applicable. High-accuracy results for large-scale crack problems are shown in [17,12] and impressive numerical experiments for the well-known problem of determining the electrostatic conductivity of a "random checkerboard" are presented in [15]. The compressed inverse preconditioning scheme is a technique for simultaneously accelerating the application of matrices discretizing integral operators given over domains with singularities and overcoming the negative effects that ill-conditioning has on iterative methods. The approach of this paper is different in several respects, the most salient being that we avoid ill-conditioning entirely by forming discretizations of integral operators which capture their action on spaces of square integrable functions rather than their pointwise behavior and that our approach is direct rather than iterative.

While neither of the observations underlying this article is new, the fact that the two can be combined to yield an effective scheme for a large class of elliptic corner problems does not appear to be known (or, at least, not widely known). Moreover, our scheme deviates from standard methods in numerous respects. In Section 1, we describe integral equation formulations of the Neumann and Dirichlet problems for the Helmholtz equation and for the boundary value problem arising from scattering from the interface of two fluids. Our approach to the Dirichlet problem and to interface boundary conditions is standard; however, we introduce a new mechanism in order to treat the "spurious resonance" problem associated with Neumann boundary conditions.

Section 2 is concerned with the discretization of integral operators. The approach described there is a novel generalization of the modified Nyström scheme introduced in [4]. The standard Nyström approach to the discretization of integral equations, which calls for representing solutions of the equations by sampling their values at a collection of points, will obviously lead to conditioning problems when solutions are unbounded with respect to pointwise norms. Since integral operators given on domains with corner points are often unbounded in L^∞ norm, Galerkin type methods, which are able to capture the L^2 action of an integral operator rather than its pointwise behavior, are generally used for the class of problems considered in this article. The disadvantage of such an approach is that Galerkin discretization requires the numerical evaluation of many double integrals. The discretization schemes of [4] and this paper are mathematically equivalent to Galerkin discretization but avoid this difficulty. They differ in that the scheme of [4] is only able to address integral operators whose kernels are smooth, while the approach of Section 2 applies to operators with logarithmically singular kernels.

In Section 3, we describe a mechanism for accelerating the numerical solution of the integral equations treated in this article. It is based on the "scattering matrix" formulation of physics. Approaches of this type have been described in [28,22,13]. Our scheme differs from previous algorithms in several respects, the most notable being that our approach explicitly incorporates user-supplied assumptions about boundary data and the desired outputs.

Finally, Section 4 presents the results of numerical experiments conducted to assess the approach of this article.

1. Three boundary value problems of scattering theory

In this section, we formulate three of the boundary value problems of scattering theory as integral equations. With the exception of the formulation used in Section 1.2, these formulations are well known. We include them for the reader's convenience and so that we may reference them later in this article.

1.1. Sound-soft scattering

Sound-soft scattering from an obstacle $\Omega \subset \mathbb{R}^2$ can be modeled through the boundary value problem

$$\begin{aligned} &\Delta u + \omega^2 u = 0 \text{ in } \Omega^c \\ &u = g \text{ on } \partial\Omega \\ &\sqrt{|x|}\left(\frac{\partial}{\partial |x|} - i\omega\right) u(x) \to 0 \text{ as} |x| \to \infty. \end{aligned} \tag{1.1}$$

This problem can be reduced to an integral equation on $\partial\Omega$ by representing the solution u of (1.1) as

$$u(x) = \frac{i}{4}\int_{\partial\Omega} \omega|x-y| H_1(\omega|x-y|)\frac{(x-y)\cdot\eta_y}{|x-y|^2}\sigma(y)ds(y) + \frac{i}{4}\int_{\partial\Omega} H_0(\omega|x-y|)\sigma(y)ds(y). \tag{1.2}$$

Here, H_0 and H_1 are the Hankel functions of the first kind of order 0 and 1, ds refers to the arclength measure on the curve $\partial\Omega$, and η_y is the outward-pointing unit normal to $\partial\Omega$ at the point y. This representation leads to the integral equation

$$\frac{1}{2}\sigma(x)+\frac{i}{4}\int_{\partial\Omega}\omega|x-y|H_1(\omega|x-y|)\frac{(x-y)\cdot\eta_y}{|x-y|^2}\sigma(y)ds(y)+\frac{i}{4}\int_{\partial\Omega}H_0(\omega|x-y|)\sigma(y)ds(y)=g(x),x\in\partial\Omega. \tag{1.3}$$

That is, the solution σ of the Eq. (1.3) is the charge distribution which, when inserted into (1.2), yields the solution u of (1.1).

Eq. (1.3), which is often referred to as a combined field integral equation due to the presence of terms involving both the single and double layer acoustic potentials, is uniquely solvable for appropriately chosen g (see, for instance, [11]). Indeed, obtaining unique solvability is the motivation for the two-term representation (1.2) of the solution u. When the solution is represented as

$$u(x)=\frac{i}{4}\int_{\partial\Omega}\omega|x-y|H_1(\omega|x-y|)\frac{(x-y)\cdot\eta_y}{|x-y|^2}\sigma(y)ds(y)$$

in analogy with the standard approach for Laplace's equation, the resulting integral equation

$$\frac{1}{2}\sigma(x)+\frac{i}{4}\int_{\partial\Omega}\omega|x-y|H_1(\omega|x-y|)\frac{(x-y)\cdot\eta_y}{|x-y|^2}\sigma(y)ds(y)=g(x),\quad x\in\partial\Omega, \tag{1.4}$$

is not uniquely solvable in $L^2(\partial\Omega)$ for all wavenumbers ω. It is, however, alway solvable — the issue is that for certain wavenumbers ω, which depend on the curve $\partial\Omega$, the operator

$$T\sigma(x)=\frac{1}{2}\sigma(x)+\frac{i}{4}\int_{\partial\Omega}\omega|x-y|H_1(\omega|x-y|)\frac{(x-y)\cdot\eta_y}{|x-y|^2}\sigma(y)ds(y) \tag{1.5}$$

can have a nontrivial nullspace. The addition of a single-layer term to (1.5) is one way to perturb the spectrum of the operator T so as to eliminate the nullspace.

1.2. Sound-hard scattering

The Neumann boundary value problem

$$\begin{aligned}&\Delta u+\omega^2u=0 \text{ in } \Omega^c\\ &\frac{\partial u}{\partial\eta}=g \text{ on } \partial\Omega\\ &\sqrt{|x|}\left(\frac{\partial}{\partial|x|}-i\omega\right)u(x)\to 0 \text{ as } |x|\to\infty.\end{aligned} \tag{1.6}$$

models sound-hard scattering from the obstacle Ω. Here, η refers to the outward-pointing unit normal of $\partial\Omega$ and the condition on the normal derivative of u is to be understood as a nontangential limit. As in the case of the Dirichlet problem, the representation of the solution u as

$$u(x)=\frac{i}{4}\int_{\partial\Omega}H_0(\omega|x-y|)\sigma(y)ds(y)$$

in analogy with the standard approach for Laplace's equation leads to the integral equation

$$-\frac{1}{2}\sigma(x)+\frac{i}{4}\int_{\partial\Omega}\omega|x-y|H_1(\omega|x-y|)\frac{(y-x)\cdot\eta_x}{|x-y|^2}\sigma(y)ds(y)=g(x),\ x\in\partial\Omega,$$

which is not necessarily uniquely solvable in $L^2(\partial\Omega)$. Once again, for certain values of ω, the associated integral operator has a nontrivial nullspace.

A combined layer representation of u of the form (1.2) is unsuitable because it results in an integral equation one term of which is a multiple of the operator

$$H\sigma(x)=\int_{\partial\Omega}\left(\frac{\partial}{\partial\eta_x}\frac{\partial}{\partial\eta_y}H_0(\omega|x-y|)\right)\sigma(y)ds(y), \tag{1.7}$$

which is not bounded $L^2(\partial\Omega)\to L^2(\partial\Omega)$. It is standard practice to instead use a representation of the solution u of (1.6) which involves a composition of integral operators. Modifications of this type can be used to obtain integral equations whose associated operators are well-conditioned on various function spaces. The use of a composition to "regularize" a hypersingular integral operator goes back at least to [24]; a more recent treatment can be found in [10].

We take a somewhat different tack and represent the solution u of (1.6) as

$$u(x)=\frac{i}{4}\int_{\partial\Omega}H_0(\omega|x-y|)\sigma(y)ds(y)+\frac{i}{4}\int_{\Gamma}H_0(\omega|x-y|)\tau(y)ds(y) \tag{1.8}$$

where Γ is a simply closed contour contained in the interior of Ω and τ is a newly introduced auxiliary charge distribution on Γ. This yields the equation

$$-\frac{1}{2}\sigma(x)+\frac{i}{4}\int_{\partial\Omega}\omega|x-y|H_1(\omega|x-y|)\frac{(y-x)\cdot\eta_x}{|x-y|^2}\sigma(y)ds(y)+\frac{i}{4}\int_{\Gamma}\omega|x-y|H_1(\omega|x-y|)\frac{(y-x)\cdot\eta_x}{|x-y|^2}\tau(y)ds(y)$$
$$=g(x),\quad x\in\partial\Omega, \tag{1.9}$$

in the unknowns σ and τ, which is not uniquely solvable. However, this problem can be easily overcome by requiring that

$$-\frac{1}{2}\tau(x)+\frac{i}{4}\int_{\Gamma}\omega|x-y|H_1(\omega|x-y|)\frac{(y-x)\cdot\eta_x}{|x-y|^2}\tau(y)ds(y)$$
$$+\frac{i}{4}\int_{\partial\Omega}\omega|x-y|H_1(\omega|x-y|)\frac{(y-x)\cdot\eta_x}{|x-y|^2}\sigma(y)ds(y)=0,\quad x\in\Gamma. \tag{1.10}$$

In the case of a domain with m connected components, we add auxiliary contours $\Gamma_1,\ldots,\Gamma_m$, one in the interior of each connected component, introduce auxiliary charge distributions $\tau_1,\ldots,\tau_m$ on the Γ_j, and add m conditions of the form (1.10), one for each connected component.

The condition numbers of the linear systems which result from the discretization of (1.9) and (1.10) are typically small at low wavenumbers. For instance, Table 1 shows the condition numbers of certain linear systems obtained by applying this approach to unit circle U. The chosen wavenumbers ω are high-accuracy approximations of roots of the Bessel function $J_1(z)$ of the first kind of order 1. It is well known that the integral operator

$$T\sigma(x)=\frac{1}{2}\sigma(x)+\frac{i}{4}\int_{U}\omega|x-y|H_1(\omega|x-y|)\frac{(y-x)\cdot\eta_x}{|x-y|^2}\sigma(y)ds(y)$$

has a nontrivial nullspace when ω takes on one of these values.

Remark 1.1. The operator H defined by (1.7) is unbounded $L^2(\partial\Omega)\to L^2(\partial\Omega)$, but it is bounded as an operator $W^{1,2}(\partial\Omega)\to L^2(\partial\Omega)$, where $W^{1,2}(\partial\Omega)$ is the Sobolev space of square integral functions f on $\partial\Omega$ whose first derivatives with respect to arclength measure are also square integrable. Indeed, H can be viewed as a linear combination of the derivative of the Hilbert transform and an integral operator whose kernel is smooth (see [19], for instance).

An integral equation method for electromagnetic scattering problems which exploits the boundedness of H on Sobolev spaces is described in [2]. Moreover, the approach of the next section to discretizing integral operators defined on spaces of square integrable functions can be modified so as to exploit this observation and produce discretizations of the operator H which are well-conditioned. A scheme of this type will be reported at a later date.

1.3. Fluid interfaces

In order to formulate the boundary value problem

$$\begin{aligned}
&\Delta u+\omega_1^2u=0 && \text{in } \Omega\\
&\Delta v+\omega_2^2v=0 && \text{in } \Omega^c\\
&u-v=g && \text{on } \partial\Omega\\
&\tfrac{\partial u}{\partial\eta}-\tfrac{\partial v}{\partial\eta}=\tfrac{\partial g}{\partial\eta} && \text{on } \partial\Omega\\
&\sqrt{|x|}\left(\tfrac{\partial}{\partial|x|}-i\omega_2\right)v(x) && \to 0 \text{ as } |x|\to\infty,
\end{aligned} \qquad \textit{xmllabele0050} \tag{1.11}$$

which models scattering from an interface between two fluids, as an integral equation we follow the approach of [25]. That is, we represent u as

$$u=D_{\omega_1}\sigma+S_{\omega_1}\tau$$

and v as

$$v=D_{\omega_2}\sigma+S_{\omega_2}\tau,$$

Table 1
The condition numbers of the linear systems obtained by applying the approach of Section 1.2 to the unit circle, as a function of wavenumber.

ω	κ	ω	κ
3.831705970207512	$9.15\times10^{+00}$	82.46225991437356	$7.07\times10^{+01}$
10.17346813506272	$9.13\times10^{+00}$	161.0042944053620	$5.73\times10^{+02}$
22.76008438059277	$9.25\times10^{+00}$	201.8454701561909	$4.01\times10^{+02}$
41.61709421281445	$1.71\times10^{+01}$	321.2266814345928	$3.61\times10^{+02}$

where S_ω and D_ω are defined by

$$S_\omega f(x) = \frac{i}{4}\int_{\partial\Omega} H_0(\omega|x-y|)f(x)ds(y)$$

and

$$D_\omega f(x) = \frac{i}{4}\int_{\partial\Omega} \omega|x-y|H_1(\omega|x-y|)\frac{(x-y)\cdot\eta_y}{|x-y|^2}f(y)ds(y).$$

This choice of representations leads to the system of integral equations

$$\begin{pmatrix} D_{\omega_1} - D_{\omega_2} - I & S_{\omega_1} - S_{\omega_2} \\ D'_{\omega_1} - D'_{\omega_2} & S'_{\omega_1} - S'_{\omega_2} + I \end{pmatrix}\begin{pmatrix}\sigma\\ \tau\end{pmatrix} = \begin{pmatrix} g \\ \frac{\partial g}{\partial \eta}\end{pmatrix}. \tag{1.12}$$

Here, S'_ω and D'_ω are the operators defined by

$$S'_\omega f(x) = \frac{i}{4}\int_{\partial\Omega} \omega|x-y|H_1(\omega|x-y|)\frac{(y-x)\cdot\eta_x}{|x-y|^2}f(y)ds(y)$$

and

$$D'_\omega f(x) = \frac{i}{4}\int_{\partial\Omega} \left(\frac{\partial}{\partial v_x}\frac{\partial}{\partial v_y}H_0(\omega|x-y|)\right)f(y)ds(y).$$

Note that due to cancellation of singularities, the operators in each entry of the matrix appearing in (1.12) are bounded $L^2(\partial\Omega) \to L^2(\partial\Omega)$.

2. Discretization of integral operators

Here we describe a Nyström scheme for the discretization of certain integral operators given over planar domains with corners. Throughout we view our operators as acting on spaces of square integrable functions and our aim is to discretize them as such. This is a departure from the standard Nyström approach which proceeds by approximating the *pointwise* action of an integral operator. Such an approach is contraindicated when considering integral operators on Lipschitz domains as they tend to be unbounded with respect to pointwise (Hölder and L^∞) norms but bounded with respect to L^p norms.

Much has been written on the analysis of integral operators on Lipschitz domains; see [9] for a treatise on the subject written by two of its leading practitioners. The article [4] contains a detailed discussion of the pitfalls encountered when standard Nyström discretization methods are applied to integral operators on Lipschitz domains.

2.1. Decompositions of planar curves

For our purposes, a decomposition of a planar curve Γ is a finite sequence

$$\{r_j : I_j \to \Gamma\}_{j=1}^n$$

of smooth unit speed parameterizations each of which is given on a compact interval I_j of $\mathbb{R}$ and such that the sets $r_j(I_j)$ form a disjoint union of Γ. By smooth parameterization $r{:}I \to \Gamma$, we mean a parameterization such that $r'(t)$ is defined for each point t in the interior of the compact interval I and that the limit of $|r'(t)|$ as t goes to the endpoints of I exists and is finite. Unit speed refers to that requirement that $|r'(t)| = 1$ for all t in the interior of I. We now associate with each decomposition of Γ a subspace S of the space $L^2(\Gamma)$ of measurable functions on Γ which are square integrable with respect to arclength measure and an isomorphism of S with a complex Cartesian space. This construction will be the basis of our approach to discretization.

To that end, we fix a positive integer k and let, for each $j = 1, \ldots, n$,

$$t_{1,j}, t_{2,j}, \ldots, t_{k,j}, w_{1,j}, w_{2,j}, \ldots, w_{k,j}$$

denote the nodes and weights of the k-point Legendre quadrature rule on the interval I_j. We also define, for each $j = 1, \ldots, n$, S_j to be the span of all functions $f : \Gamma \to \mathbb{C}$ of the form

$$f(x) = \begin{cases} p\left(r_j^{-1}(x)\right) & \text{for } x \in r_j(I_j) \\ 0 & \text{for } x \notin r_j(I_j)\end{cases}$$

where p is a Legendre polynomial of degree $k-1$ on I_j. The mapping

$$\Phi_j : S_j \subset L^2(\Gamma) \to \mathbb{C}^k$$

defined by

$$\Phi_j(f) = \begin{pmatrix} f(r_j(t_{1,j}))\sqrt{w_{1,j}} \\ f(r_j(t_{2,j}))\sqrt{w_{2,j}} \\ \vdots \\ f(r_j(t_{k,j}))\sqrt{w_{k,j}} \end{pmatrix}$$

is evidently an isomorphism: if f and g are in the space S_j then we have

$$\int_\Gamma fg = \int_{r_j(I_j)} fg = \int_{I_j} f(r_j(t))g(r_j(t))dt = \sum_{i=1}^{k} f(r_j(t_{i,j}))g(r_j(t_{i,j}))\sqrt{w_{i,j}} = \Phi(f)\cdot\Phi(g).$$

The third equality follows from the fact that the functions

$$f \circ r_j \text{ and } g \circ r_j$$

are Legendre polynomials of degree $k-1$ on I_j and the Legendre quadrature rule of order k on I_j integrates products of all such functions. The subspace S is now defined as the union of the subspaces S_j and the map

$$\Phi : S \to (\mathbb{C}^k)^n \equiv \mathbb{C}^{kn}$$

is obtained by setting

$$\Phi(f) = \begin{pmatrix} \Phi_1(f_1) \\ \Phi_2(f_2) \\ \vdots \\ \Phi_n(f_n) \end{pmatrix},$$

where f_j denotes the restriction of f to $r_j(I_j)$. Finally, we introduce two pieces of terminology which will be useful later. We will refer to the points

$$r_1(t_{1,1}), r_1(t_{2,1}), \ldots, r_1(t_{k,1}), \ldots, \quad r_n(t_{1,n}), r_n(t_{2,n}), \ldots, r_n(t_{k,n}) \tag{2.1}$$

as the discretization nodes of the decomposition. And, given a function f on Γ which is defined at these nodes, we call the unique function g in S such that

$$f(r_j(t_{i,j})) = g(r_j(t_{i,j})), \quad i = 1,\ldots,k, \quad j = 1,\ldots,n,$$

the interpolant of f in S.

Remark 2.1. The requirement that the parameterizations r_j be unit speed can be dropped. In that event, the definition of Φ_j should be modified to read

$$\Phi_j(f) = \begin{pmatrix} f(r_j(t_{1,j}))\sqrt{w_{1,j}|r_j'(t_{1,j})|} \\ f(r_j(t_{2,j}))\sqrt{w_{2,j}|r_j'(t_{2,j})|} \\ \vdots \\ f(r_j(t_{k,j}))\sqrt{w_{k,j}|r_j'(t_{k,j})|} \end{pmatrix}$$

and the definition of the S_j must be adjusted accordingly.

2.2. Discretization of operators acting on spaces of square integrable functions

A decomposition

$$D = \{r_j : I_j \to \Gamma\}_{j=1}^n$$

of a planar curve Γ gives rise to a scheme for the discretization of certain operators $T: L^2(\Gamma) \to L^2(\Gamma)$, which we now describe. We denote by S and by $\Phi : S \to \mathbb{C}^{nk}$ the subspace of $L^2(\Gamma)$ and the isomorphism associated with the decomposition D.

Moreover, we let P designate the mapping which takes functions f which are defined at the discretization nodes of the decomposition to their interpolants in S; that is, $P(f)$ is the unique function g in S which agrees with f at the nodes (2.1). If $T:L^2(\Gamma) \to L^2(\Gamma)$ is such that Tf is defined at each of the discretization nodes of D whenever f is a function in S, then we call the $nk \times nk$ matrix A such that the diagram

$$\begin{array}{ccc} S \subset L^2(\Gamma) & \xrightarrow{PT} & S \subset L^2(\Gamma) \\ \downarrow \Phi & & \downarrow \Phi \\ \mathbb{C}^{nk} & \xrightarrow{A} & \mathbb{C}^{nk} \end{array} \tag{2.2}$$

commutes the discretization of the operator T induced by the decomposition D. The salient feature of this definition is that that the singular values of A are identical to those of the operator PT. It follows that the $l^2(\mathbb{C}^{nk}) \to l^2(\mathbb{C}^{nk})$ condition number of the matrix A is equal to the $L^2(\Gamma) \to L^2(\Gamma)$ condition number of the operator PT. Many of the integral operators of mathematical physics are well-conditioned when viewed as operators on spaces of square integral functions but are not well-behaved with respect to pointwise norms. This is certainly true of the operators which arise from the formulations of Section 1 when considered on Lipschitz domains. They are typically unbounded on Hölder spaces but are bounded on spaces of square integrable functions (see [9], for instance).

In a similar vein, decompositions of two disjoint contours Γ_1 and Γ_2 give rise to a scheme for discretizing certain operators $T:L^2(\Gamma_1) \to L^2(\Gamma_2)$. Denote by

$$\Phi_1 : S_1 \subset L^2(\Gamma_1) \to \mathbb{C}^{nk}$$

the isomorphism associated with the decomposition of Γ_1 and by

$$\Phi_2 : S_2 \subset L^2(\Gamma_2) \to \mathbb{C}^{mk}$$

the isomorphism associated with Γ_2. Moreover, let P_2 be the operator taking functions f defined on Γ_2 to their interpolants in S_2. If $T:L^2(\Gamma_1) \to L^2(\Gamma_2)$ has the property that Tf is pointwise defined at the discretization nodes of Γ_2 whenever f is a function in S_1, then we say the $mk \times nk$ matrix

$$\Phi_2 P_2 T \Phi_1^{-1}$$

is the discretization of T arising from the given decompositions of Γ_1 and Γ_2. In other words, the discretization of T is the matrix B such that

$$\begin{aligned} \Delta u + \omega^2 u &= 0 \quad \text{in } \Omega^c \\ u &= g \quad \text{on } \partial\Omega \\ \sqrt{|x|}\left(\frac{\partial}{\partial |x|} - i\omega\right) u(x) &\to 0 \text{ as } |x| \to \infty. \end{aligned}$$

commutes.

2.3. Numerical approximation of matrices discretizing a class of integral operators

We now describe a method for the numerical approximation of the entries of the matrix A defined by the diagram (2.2) in the event that $T:L^2(\Gamma) \to L^2(\Gamma)$ is an integral operator

$$Tf(x) = \int_\Gamma K(x,y) f(y) ds(y)$$

whose kernel is of the form

$$K(x,y) = \log|x-y| f(x,y) + g(x,y)$$

with f and g smooth functions $\Gamma \times \Gamma \to \mathbb{C}$. For $j = 1, \ldots, n$ and $i = 1, \ldots, k$ set

$$x_{ij} = r_j(t_{ij}),$$

where $t_{1j}, \ldots, t_{kj}$ once again denote the nodes of the k-point Legendre quadrature rule on the interval I_j. Also, for $j = 1, \ldots, n$, let

$$w_{1j}, w_{2j}, \ldots, w_{kj}$$

be the weights of the k-point Legendre quadrature formula on the interval I_j. Then the matrix A is obviously the mapping which takes the scaled values

$$f(x_{ij})\sqrt{w_{ij}}, \quad i = 1, \ldots, k, \quad j = 1, \ldots, n$$

of the function f to the scaled values

$$\int_\Gamma \sqrt{w_{i,j}} K(x_{i,j}, y) f(y) ds(y), i = 1, \ldots, k, j = 1, \ldots, n \tag{2.3}$$

of the function Tf. Each of the integrals in (2.3) can be decomposed as

$$\sum_{s=1}^{n} \int_{r_s(I_s)} \sqrt{w_{i,j}} K(x_{i,j}, y) f(y) ds(y)$$

and it is in this form that we will evaluate them. That is, we will show how to evaluate

$$\int_{r_s(I_s)} \sqrt{w_{i,j}} K(x_{i,j}, y) f(y) ds(y),$$

where $x_{i,j}$ is a discretization node on one of the contours $r_j(I_j)$ and $w_{i,j}$ is the corresponding quadrature weight, using the scaled values

$$f(x_{1,s})\sqrt{w_{1,s}}, \ldots, f(x_{k,s})\sqrt{w_{k,s}}$$

of f at the discretization nodes on a "source" contour $r_s(I_s)$. The discretization matrix A can plainly be formed using this construction.

In the event that $x_{i,j}$ is distant from the interval $r_s(I_s)$, the relevant integral can be approximated as

$$\int_{r_s(I_s)} \sqrt{w_{i,j}} K(x_{i,j}, y) f(y) ds(y) \approx \sum_{l=1}^{k} K(x_{i,j}, x_{l,s}) \sqrt{w_{i,j}} \sqrt{w_{l,s}} (f(x_{l,s}) \sqrt{w_{l,s}});$$

that is, using the Legendre quadrature formula on the interval I_s. For the solver of this paper, a bounding circle C_s is found for each of the contours $r_s(I_s)$ and a point x is considered sufficiently distant from $r_s(I_s)$ if x is in the exterior of the circle $2C_s$.

If the node $x_{i,j}$ is within the annulus $2C_s \backslash C_s$, then we use a specialized "near" quadrature rule to perform the necessary evaluation. In particular, we make use of a quadrature formula of the form

$$\int_{-1}^{1} \log|t - y| f(y) + g(y)\ ds(y) \approx \sum_{l=1}^{m} (\log|t - z_l| f(z_l) + g(z_l)) v_l \tag{2.4}$$

which holds when g and f are polynomials of degree $2k$ and t is either a point in $[-2, -1] \cup [1,2]$ or on the circle of radius 1.1 centered at 0. Quadratures of this type can be constructed using the algorithm of [5]. The integral

$$\int_{r_s(I_s)} \sqrt{w_{i,j}} K(x_{i,j}, y) f(y) ds(y)$$

is evaluated by first interpolating the function f from its scaled values at the nodes $x_{1,s}, \ldots, x_{k,s}$ to its scaled values at $r_s(z_1), \ldots, r_s(z_m)$; that is, the quantities

$$f(x_{1,s})\sqrt{w_{1,s}}, \ldots, f(x_{k,s})\sqrt{w_{k,s}}$$

are used to compute

$$f(r_s(z_1))\sqrt{v_1}, \ldots, f(r_s(z_m))\sqrt{v_m}. \tag{2.5}$$

The $m \times k$ matrix which performs this mapping can be constructed quite easily. Indeed, if

$$t_1, \ldots, t_k, w_1, \ldots, w_k$$

are the nodes and weights of the k-point Legendre quadrature rule on the interval $[-1,1]$ and $p_0, \ldots, p_{k-1}$ denote the normalized Legendre polynomials of degree 0 through $k-1$ on $[-1,1]$, then the relevant matrix is simply

$$\begin{pmatrix} p_0(z_1)\sqrt{v_1} & \cdots & p_{k-1}(z_1)\sqrt{v_1} \\ p_0(z_2)\sqrt{v_2} & \cdots & p_{k-1}(z_2)\sqrt{v_2} \\ \vdots & \ddots & \vdots \\ p_0(z_m)\sqrt{v_m} & \cdots & p_{k-1}(z_m)\sqrt{v_m} \end{pmatrix} \begin{pmatrix} p_0(t_1)\sqrt{w_1} & \cdots & p_0(t_k)\sqrt{w_k} \\ p_1(t_1)\sqrt{w_1} & \cdots & p_1(t_k)\sqrt{w_k} \\ \vdots & \ddots & \vdots \\ p_{k-1}(t_1)\sqrt{w_1} & \cdots & p_{k-1}(t_k)\sqrt{w_k} \end{pmatrix}. \tag{2.6}$$

The formula (2.4) can be used to approximate the desired integral from the values (2.5). Note that both of the matrices appearing in (2.6) have orthogonal columns. This follows from the fact that the quadrature rules $t_1, \ldots, t_k, w_1, \ldots, w_k$ and $z_1, \ldots, z_m, v_1, \ldots, v_m$ integrate products of the Legendre polynomials of degree $k-1$ on $[-1,1]$. As a consequence, the singular values of the interpolation matrix are all either 1 or 0.

When the target $x_{i,j}$ is one of the nodes $x_{1,s}, \ldots, x_{k,s}$ on the source contour $r_s(I_s)$, the procedure used to evaluate the integral

$$\int_{r_s(I_s)} \sqrt{w_{i,j}} K(x_{i,j}, y) f(y) ds(y)$$

is almost identical to that just described. The only difference is that quadratures for integrals of the form

$$\int_{-1}^{1} \log|t_i - y| f(y) + g(y)\ ds(y),$$

where f and g are polynomials of degree $2k$ and t_i is one of the nodes of the k-point Legendre quadrature rule, are used in place of (2.4). The necessary quadrature rules can be constructed using the approach of [5].

Remark 2.2. The algorithm of this section can plainly be used to discretize an operator

$$T : L^2(\Gamma_1) \rightarrow L^2(\Gamma_2)$$

which maps square integrable functions on the contour Γ_1 to square integral functions on a contour Γ_2 which is disjoint from Γ_1 provided that T is of the form

$$Tf(x) = \int_{\Gamma_1} K(x,y) f(y) ds(y)$$

with K as in (2.3).

Remark 2.3. It is well known that

$$H_0(z) = \frac{2i}{\pi} \log\left(\frac{z}{2}\right) J_0(z) + f(z), \tag{2.7}$$

where $J_0(z)$ is the Bessel function of the first kind of order 0 and $f(z)$ is analytic. This fact can be used to obtain an alternate approach to evaluating integrals involving the Hankel functions H_0 and H_1. In particular, it allows us to write the integrands as

$$\log|x - y| k_1(x,y) + k_2(x,y)$$

with k_1 and k_2 smooth functions which can be evaluated at arbitrary points. Quadrature rules for smooth functions and for integrals of the form

$$\int_{-1}^{1} \log|z - x| \left(\sum_{j=1}^{n} \alpha_j P_j(x) \right) dx, \tag{2.8}$$

where P_j denotes the Legendre polynomial of degree j and z is a fixed point in $\mathbb{C} \notin \{-1, 1\}$, can then be used to evaluate the integrals. A quadrature rule $x_1, \ldots, x_n, w_1, \ldots, w_n$ for functions of the form (2.8) can be formed by letting $x_1, \ldots, x_n$ be the nodes of the n-point Legendre quadrature and constructing weights with the help of the formula

$$\int_{-1}^{1} \log|z - x|\ P_n(x) dx = \frac{2Q_{n+1}(z) - 2Q_n(z)}{2n+1}. \tag{2.9}$$

Here, Q_n denotes the Legendre function of the second kind of order n. The branch cuts of Q_n must be chosen depending on the location of z in order to make formula (2.9) hold. See Chapter 12 of [21] for a similar approach.

Remark 2.4. In order to simplify the discussion in this section, we have made the assumption that the entire matrix A is being formed at once. However, the procedure described here can be trivially modified so as to obtain a method for the evaluation of individual entries of the matrix A. All of the experiments of Section 4 were carried out using a modified procedure with this property.

3. Scattering matrices as a tool for accelerating numerical calculations

The reduction of a boundary value problem to an integral equation does not immediately yield a computationally feasible scheme for its solution. The discretization of an integral equation typically results in a dense system of linear equations and in most cases, the direct solution of the system is prohibitively expensive. Iterative methods can improve the situation considerably, but by themselves they still fall far short of what is required for large-scale problems.

In the 1980s, a number of fast solvers for integral equations were introduced. These first generation solvers, the most prominent of which are the various fast multipole methods described in [26–28], are schemes for the rapid application of the matrices arising from the discretization of certain classes of integral operators. When combined with an iterative method for solving linear systems, like the GMRES algorithm, such a scheme allows for the rapid solution of integral equations. The limitations of first generation solvers are well known by now: the number of iterations required and the accuracy of the

obtained solution are sensitive to the condition number of the linear system and they are not particularly effective for problems involving many right-hand sides.

A second generation of fast solvers for integral equations that address many of the shortcomings of iterative methods emerged in the early part of the last decade. These new solvers, generally referred to as fast direct solvers, proceed by producing compressed representations of the inverses of matrices discretizing integral equations. Because the approach is direct rather than iterative, these solvers are much more resistant to ill-conditioning then earlier solvers. Moreover, once a coefficient matrix has been processed, the linear system of equations associated with it can be solved efficiently for many right-hands sides. Many variants of this approach have now been described in the literature; the solver we now describe is similar to those described in [22,13].

In order to simplify this discussion, we will limit ourselves to the exterior Dirichlet problem (1.1). In typical scattering problems, the boundary data g will be a potential emanating from some collection of sources outside of the domain Ω. Likewise, we are usually only interested in the values of the solution u at some distance from the domain Ω. Our solver takes advantage of these facts by requiring that the user make the possible inputs to the problem and the desired outputs explicit. More specifically, the user must specify a contour Γ_{in} such that the boundary data g in (1.1) is in the image of the operator $T_{\text{in}}: L^2(\Gamma_{\text{in}}) \rightarrow L^2(\partial\Omega)$ defined by

$$T_{\text{in}} f(x) = \frac{i}{4} \int_{\Gamma_{\text{in}}} H_0(\omega|x-y|) f(y) ds(y) \tag{3.1}$$

and a contour Γ_{out} such that the desired output for the problem is the image of the charge distribution σ which is solution of Eq. (1.3) under the operator $T_{\text{out}}: L^2(\partial\Omega) \rightarrow L^2(\Gamma_{\text{out}})$ defined by

$$T_{\text{out}} f(x) = \frac{i}{4} \int_{\partial\Omega} H_0(\omega|x-y|) f(y) ds(y) + \frac{i}{4} \int_{\partial\Omega} \omega|x-y| H_1(\omega|x-y|) \frac{(x-y)\cdot\eta_y}{|x-y|^2} f(y) ds(y). \tag{3.2}$$

Note that if Γ_{out} is a simple closed curve enclosing the domain Ω, then the values of u on the exterior of Γ_{out} are determined by its values on the contour Γ_{out}. Similarly, if Γ_{in} is a simple closed curve, then potentials generated by sources in the non-compact domain bounded by Γ_{in} are in the image of T_{in}.

We would like to form an operator which takes any g in the image of T_{in} to a charge distribution σ on $\partial\Omega$ such that $T_{\text{out}}\sigma$ agrees with the solution u of (1.1) on Γ_{out}. There is a unique operator with this property: the inverse $T_{\partial\Omega}^{-1}$ of the operator $T_{\partial\Omega}: L^2(\partial\Omega) \rightarrow L^2(\partial\Omega)$ defined by

$$T_{\partial\Omega} f(x) = \frac{1}{2} f(x) + \frac{i}{4} \int_{\partial\Omega} H_0(\omega|x-y|) f(y) ds(y) + \frac{i}{4} \int_{\partial\Omega} \omega|x-y| H_1(\omega|x-y|) \frac{(x-y)\cdot\eta_y}{|x-y|^2} f(y) ds(y). \tag{3.3}$$

However, since the singular values of the operator $T_{\partial\Omega}^{-1}$ are bounded away from zero, there is no finite-dimensional operator which accurately approximates it. But due to the compactness of T_{in} and T_{out}, there exist many compact operators $S: L^2(\partial\Omega) \rightarrow L^2(\partial\Omega)$ such that

$$\|T_{\text{out}} S T_{\text{in}} - T_{\text{out}} T_{\partial\Omega}^{-1} T_{\text{in}}\|_2 < \epsilon. \tag{3.4}$$

We call an operator S with this property an ϵ-scattering matrix. The output of our solver will be a matrix which represents an operator S with this property. We will make precise the exact nature of the inputs and outputs of our algorithm in what follows.

Remark 3.1. In many of the numerical experiments of this paper, Γ_{in} is taken to be a contour inside of the domain Ω under consideration rather than a contour enclosing it. This is because it is quite simple to construct known solutions to the boundary value problems of Section 1 in this fashion. In typical scattering problems, the incoming potentials are generated by sources outside of the domain.

3.1. Discretization of the problem

We now begin the description of the algorithm proper with a discussion of the discretization of the operators introduced above. Our algorithm takes as input a precision $\epsilon_0 > 0$, a decomposition for $\partial\Omega$, and decompositions for the two contours Γ_{in} and Γ_{out}. Let $A_{\partial\Omega}$ denote the discretization of the operator $T_{\partial\Omega}$ induced by the given decomposition of $\partial\Omega$ and let A_{in} and A_{out} be the induced discretizations of T_{in} and T_{out}, respectively. The output of the algorithm will be a matrix S such that

$$A_{\text{out}} A_{\partial\Omega}^{-1} A_{\text{in}} \approx A_{\text{out}} S A_{\text{in}}. \tag{3.5}$$

Assuming that the given decompositions are properly chosen, a bound of the form (3.4) follows since $A_{\text{out}} A_{\partial\Omega}^{-1} A_{\text{in}}$ will be an approximation of the operator $T_{\text{out}} T_{\partial\Omega}^{-1} T_{\text{in}}$. Note, however, that the error in this approximation will not necessarily be bounded by ϵ_0. The relationship between the specified precision and the resulting error bound is quite complicated and an investigation of that relationship is beyond the scope of this paper.

Owing to the procedure used to construct them, each row or column of the matrices A_{in}, A_{out} and $A_{\partial\Omega}$ is associated with a discretization node on one of the contours Γ_{in},Γ_{out} or $\partial\Omega$. For instance, if we denote by $x_1, x_2, \ldots, x_{n_{\text{in}}}$ the discretization nodes on Γ_{in} and by $w_1, w_2, \ldots, w_{n_{\text{in}}}$ their corresponding weights and if we let y_1,y_2, … ,y_n,v_1, … ,v_n be the discretization nodes on $\partial\Omega$ and their corresponding weights, then A_{in} is the $n \times n_{n_{\text{in}}}$ matrix which maps the scaled values

$$\begin{pmatrix} f(x_1)\sqrt{w_1} \\ f(x_2)\sqrt{w_2} \\ \vdots \\ f(x_{n_{\text{in}}})\sqrt{w_{n_{\text{in}}}} \end{pmatrix}$$

of a function f in the discretization subspace associated with the decomposition of Γ_{in} to the scaled values

$$\begin{pmatrix} h(y_1)\sqrt{v_1} \\ h(y_2)\sqrt{v_2} \\ \vdots \\ h(y_n)\sqrt{v_n} \end{pmatrix}$$

of the interpolant h of $T_{\text{in}}f$ in the discretization subspace associated with the decomposition given on $\partial\Omega$. We can therefore associate rows of A_{in} with discretization nodes x_j on Γ_{in} and columns of A_{in} with discretization nodes y_j on $\partial\Omega$.

In what follows, we will often subsample the matrices A_{in}, A_{out} and $A_{\partial\Omega}$ by retaining those rows and columns associated with particular ordered sets of discretization nodes. The construction is used frequently enough that it warrants the following definition.

Let Y_{in} be an ordered set

$$y_1, y_2, \ldots, y_m$$

of discretization nodes on $\partial\Omega$ and Γ_{in}, and let X_{out} be an ordered set

$$x_1, x_2, \ldots, x_n$$

of discretization nodes on $\partial\Omega$ and Γ_{out}. We use the notation $A(X_{\text{out}},Y_{\text{in}})$ to denote the $n \times m$ matrix whose entries are obtained in the following fashion. If x_i and y_j are nodes on $\partial\Omega$ then we let A_{ij} be the entry of the matrix $A_{\partial\Omega}$ in the row corresponding to the node x_i and the column corresponding to the node y_j. If x_i is a node on Γ_{out} and y_j is a node on $\partial\Omega$, then the entry A_{ij} is taken to be the entry of A_{out} in the column corresponding to y_j and the row corresponding to x_i. Finally, if x_i is a node on $\partial\Omega$ and y_j is a node on Γ_{in}, then the entry A_{ij} is taken to be the entry of A_{in} in the row corresponding to x_i and the column corresponding to y_j. As we do not allow nodes from Γ_{out} to be in the ordered set Y_{in} and nodes from Γ_{in} to be in the ordered set X_{out}, we have exhausted all possible combinations.

Moreover, we will have occasion to introduce points on artificial "auxiliary" contours into the sets Y_{in} and X_{out}. Let Λ denote such a contour and assume a decomposition of Λ is given. Denote by $A_{\Lambda\to\partial\Omega}$ and by $A_{\partial\Omega\to\Lambda}$ the induced decompositions of the operators $T_{\Lambda\to\partial\Omega}$:$L^2(\Lambda) \to L^2(\partial\Omega)$ and $T_{\partial\Omega\to\Lambda}$:$L^2(\partial\Omega) \to L^2(\Lambda)$ given by

$$T_{\Lambda\to\partial\Omega}f(x) = \frac{i}{4}\int_{\Lambda} H_0(\omega|x-y|)f(y)ds(y) + \frac{i}{4}\int_{\Lambda} \omega|x-y|H_1(\omega|x-y|)\frac{(x-y)\cdot\eta_y}{|x-y|^2}f(y)ds(y)$$

and

$$T_{\partial\Omega\to\Lambda}f(x) = \frac{i}{4}\int_{\partial\Omega} H_0(\omega|x-y|)f(y)ds(y) + \frac{i}{4}\int_{\partial\Omega} \omega|x-y|H_1(\omega|x-y|)\frac{(x-y)\cdot\eta_y}{|x-y|^2}f(y)ds(y),$$

respectively. If $y_j \in Y_{\text{in}}$ is in Λ and $x_i \in X_{\text{out}}$ is a discretization node on $\partial\Omega$ then we take the ij entry of $A(X_{\text{out}},Y_{\text{in}})$ to be the entry in the row of $A_{\Lambda\to\partial\Omega}$ corresponding to x_i and the column corresponding to y_j. Similarly, if x_i is in Λ and y_j is a discretization node on $\partial\Omega$, then we take the ij entry of $A(X_{\text{out}},Y_{\text{in}})$ to be the entry in the row of $A_{\partial\Omega\to\Lambda}$ corresponding to x_i and the column corresponding to y_j. We could adopt the obvious extension of these definitions to the case of interactions of points in Γ_{in} and Γ_{out} with points in an auxiliary contour Λ, but no such interactions will arise.

3.2. A single-level algorithm

In this section, we describe a one-level scheme for constructing a matrix S with the property (3.5). The algorithm proceeds by first constructing an approximate factorization

$$\|A_{\text{in}} - R\widetilde{A_{\text{in}}}\| < \epsilon_0 \tag{3.6}$$

where $\widetilde{A_{\text{in}}}$ is a matrix consisting of k_{in} rows of A_{in}. A factorization of this type with k_{in} approximately equal to the numerical rank of the matrix A_{in} to precision ϵ_0 can be formed in a stable fashion using the algorithm of [14] (see [23]). Since the

factorization (3.6) samples rows of A_{in}, we can view it as as identifying an ordered set Z_{in} of discretization nodes on the contour $\partial\Omega$. Denote these nodes by

$$y_{j_1}, y_{j_2}, \ldots, y_{j_{k_{\text{in}}}}$$

and let Y be the $n \times k_{\text{in}}$ matrix with entries

$$Y_{st} = \begin{cases} 1 & s = j_t \\ 0 & \text{otherwise.} \end{cases} \tag{3.7}$$

Next, we form an approximate factorization

$$\|A_{\text{out}} - \widetilde{A_{\text{out}}} L\| < \epsilon_0 \tag{3.8}$$

where $\widetilde{A_{\text{out}}}$ consists of k_{out} columns of A_{out} with k_{out} approximately equal to the numerical rank of the matrix A_{out} to precision ϵ_0. Let Z_{out} be the ordered set

$$x_{i_1}, x_{i_2}, \ldots, x_{i_{k_{\text{out}}}}$$

of discretization nodes on the contour $\partial\Omega$ identified by the factorization (3.8) and denote by X the $k_{\text{out}} \times n$ matrix constructed in analogy with the matrix Y defined in (3.7).

The $n \times n$ matrix

$$S = YLA_{\partial\Omega}^{-1}RX$$

is the desired scattering matrix since

$$A_{\text{out}} S A_{\text{in}} = A_{\text{out}} YLA_{\partial\Omega}^{-1}RXA_{\text{in}} = \widetilde{A_{\text{out}}} LA_{\partial\Omega}^{-1}R\widetilde{A_{\text{in}}} \approx A_{\text{out}}A_{\partial\Omega}^{-1}A_{\text{in}}.$$

Because the effect of applying X to A_{out} from the right is simply to subsample and permute the columns of A_{out} and the effect of applying Y to A_{in} from the left is to do likewise to the rows of A_{in}, computations involving the matrix S can be carried out using only the $k_{\text{out}} \times k_{\text{in}}$ submatrix

$$\widetilde{S} = LA_{\partial\Omega}^{-1}R$$

of S.

Indeed, the matrix S itself is principally a notational convenience. Whenever computations involving a scattering matrix S are described, it will be assumed that those computations are performed in an efficient manner using only the submatrix $\widetilde{S}$. For instance, in order to solve the boundary value problem (1.1) using this matrix, we form the vector v whose entries are the scaled values

$$\begin{pmatrix} g(y_{j_1})\sqrt{w_{j_1}} \\ \vdots \\ g(y_{j_{k_{\text{in}}}})\sqrt{w_{j_{k_{\text{in}}}}} \end{pmatrix}$$

of the boundary data g at the points in Z_{in} and apply the matrix $\widetilde{S}$ to the vector v. This yields the scaled values

$$\begin{pmatrix} \sigma(x_{i_1})\sqrt{w_{i_1}} \\ \vdots \\ \sigma(x_{i_{k_{\text{out}}}})\sqrt{w_{i_{k_{\text{out}}}}} \end{pmatrix}$$

of a charge distribution σ which is defined at the nodes in Z_{out}. To evaluate the solution u of (1.1) at a point z we calculate sum

$$\frac{i}{4}\sum_{l=1}^{k_{\text{out}}} \left(H_0(\omega|z - x_{i_l}|)\sqrt{w_{i_l}} + \omega|z - x_{i_l}|H_1(\omega|z - x_{i_l}|)\frac{(z - x_{i_l})\cdot \eta_{x_{i_l}}}{|x - x_{i_l}|^2}\sqrt{w_{i_l}} \right) \sigma(x_{i_l})\sqrt{w_{i_l}}. \tag{3.9}$$

That is, the inputs need only be evaluated at the nodes in Z_{in}, the outputs only at the nodes in Z_{out} and only the values of the submatrix $\widetilde{S}$ of S are required to perform the computation. By construction, we are assured that the value of the sum (3.9) will approximate $u(z)$ whenever z is a discretization node on Γ_{out}. If Γ_{out} is a simple closed curve enclosing the domain Ω, then this approximation of u will be accurate for points in the exterior of Γ_{out} as well. To indicate the procedure described in this paragraph we will simply say that the scattering matrix S was applied to the incoming potential g in order to form the outgoing charge distribution σ and leave the details to the reader.

We call the set Z_{in} an incoming skeleton for the contour $\partial\Omega$ and the set Z_{out} an outgoing skeleton for $\partial\Omega$. We refer to the process by which we constructed the matrix S as the skeletonization of the contour $\partial\Omega$ and we will refer to the matrix S as a

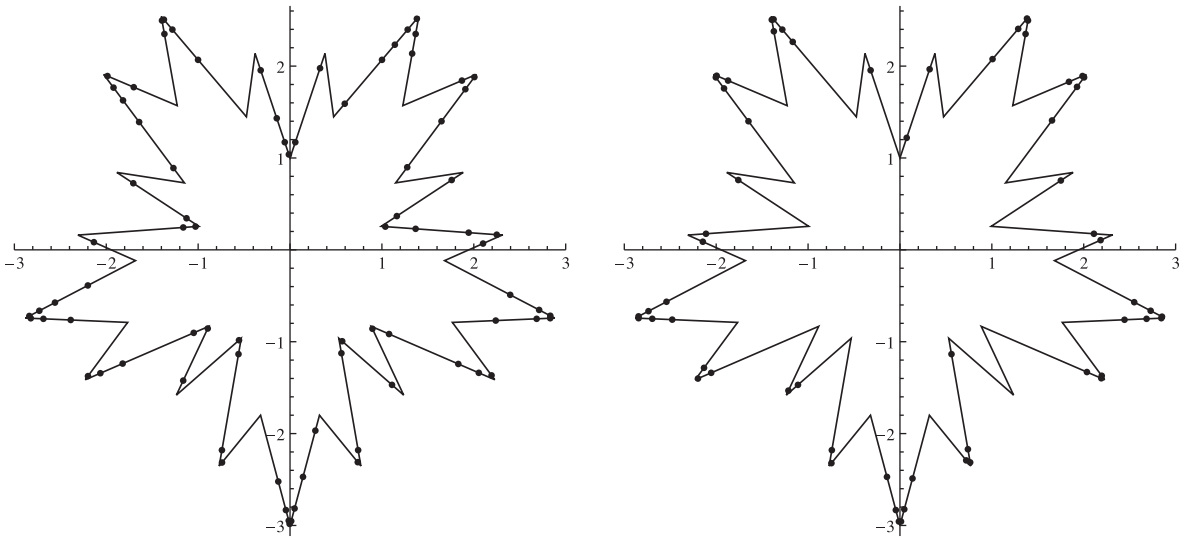

Fig. 1. The nodes of an incoming (left) and outgoing (right) skeleton on the boundary of a Lipschitz domain.

scattering matrix for $\partial\Omega$. Note that all of these objects are non-unique. Fig. 1 shows an incoming and an outgoing skeleton on the boundary of a Lipschitz domain which were constructed in the course of performing the experiments of Section 4.

Remark 3.2. The solver of this paper uses pivoted Gram-Schmidt with reorthogonalization in lieu of the algorithm of [14]. It is well known that in practice, as long as reorthogonalization is performed, the pivoted Gram-Schmidt algorithm can be substituted for the more complicated scheme of [14] with little chance of ill effects. See [3] for a discussion of the issue.

3.3. Scattering matrices for subsets of discretization nodes on $\partial\Omega$

With this section, we begin the description of a divide and conquer approach to the construction of scattering matrices. It is based on the observation that we can just as easily compute a scattering matrix for a portion of the curve $\partial\Omega$ as for $\partial\Omega$ itself.

Let $Z_{\partial\Omega}$ denote the set of all discretization nodes on $\partial\Omega$ and let Z be an ordered subset of $Z_{\partial\Omega}$. We take Y_{in} to be the union of the discretization nodes on Γ_{in} and the set $Z_{\partial\Omega}\backslash Z$. Similarly, we let X_{out} be the union of the discretization nodes on Γ_{out} and the set $Z_{\partial\Omega}\backslash Z$. A scattering matrix for Z is a matrix S such that

$$A(X_{\text{out}}, Z)A(Z, Z)^{-1}A(Z, Y_{\text{in}}) \approx A(X_{\text{out}}, Z)SA(Z, Y_{\text{in}}).$$

A matrix S with this property can be constructed by applying the procedure of the preceding section with $A(Z,Z)$ in place of $A_{\partial\Omega}$,$A(X_{\text{out}},Z)$ in place of A_{out} and $A(Z,Y_{\text{in}})$ in place of A_{in}. In particular, approximate factorizations

$$\|A(Z, Y_{\text{in}}) - R\widetilde{A}(Z, Y_{\text{in}})\|_2 < \epsilon_0, \tag{3.10}$$

where $\widetilde{A}(Z, Y_{\text{in}})$ is a subset of the rows of $A(Z,Y_{\text{in}})$, and

$$\|A(X_{\text{out}}, Z) - \widetilde{A}(X_{\text{out}}, Z)L\|_2 < \epsilon_0, \tag{3.11}$$

where $\widetilde{A}(X_{\text{out}}, Z)$ consists of a subset of the columns of $A(X_{\text{out}},Z)$, are computed and the matrix S is taken to be

$$LA(Z, Z)^{-1}R.$$

In many instances, the necessary factorizations can be constructed rapidly. Typically, there exists a factorization of $A(X_{\text{out}},Z)$ of the form

$$A(X_{\text{out}}, Z) = BC \tag{3.12}$$

where C has significantly fewer rows than $A(X_{\text{out}},Z)$. If C can then be factored as

$$C = \widetilde{C}R,$$

where $\widetilde{C}$ consists of the columns of C with indices $i_1,i_2,\ldots,i_k$, then we have

$$A(X_{\text{out}}, Z) \approx \widetilde{A}(X_{\text{out}}, Z)R,$$

where $\widetilde{A}(X_{\text{out}}, Z)$ is the matrix consisting of the columns of $A(X_{\text{out}},Z)$ with indices $i_1,i_2,\ldots,i_k$. See [29] for a number of useful error bounds which apply to procedures of this type. Note that the matrix B need never be computed since the formation of a scattering matrix requires only that we compute the factor R and the indices $i_1,i_2,\ldots,i_k$. We call a matrix C which is used in this fashion a proxy for the matrix $A(X_{\text{out}},Z)$.

Our solver constructs a proxy for $A(X_{\text{out}},Z)$ by first forming a bounding circle Λ enclosing the points in the set Z and constructing a decomposition for 2Λ. Then, all nodes in X_{out} which are in the exterior of 4Λ are removed from Z_{out} to form a set X'_{out}. The discretization nodes on 2Λ are introduced in their place to form a set X''_{out}. The matrix C is then taken to be the matrix $A(X''_{\text{out}}, Z)$ as defined at the end of Section 3.1. Less precisely but more succinctly, target nodes outside of the contour 4Λ are replaced by a collection of target nodes on 2Λ. That a factorization of the form (3.12) exists is a consequence of elementary potential theory. Of course, an analogous procedure is used to efficiently factor the matrix $A(Z,Y_{\text{in}})$.

3.4. The combination of scattering matrices

Suppose that S_1 and S_2 are scattering matrices for ordered subsets Z_1 and Z_2 of the set $Z_{\partial\Omega}$ of discretization nodes on $\partial\Omega$. Then it can be shown by elementary manipulation that the matrix

$$\begin{pmatrix} I & -S_1A(Z_1,Z_2) \\ -S_2A(Z_2,Z_1) & I \end{pmatrix}^{-1} \begin{pmatrix} S_1 & 0 \\ 0 & S_2 \end{pmatrix} \tag{3.13}$$

is a scattering matrix for $Z_1 \times Z_2$, which we can identify with the union $Z_1 \cup Z_2$. Of course, the scattering matrix formed in this fashion is suboptimal because we have just combined the incoming skeletons on Z_1 and Z_2 to form an incoming skeleton Z_{in} for the their union and similarly with the outgoing skeleton Z_{out}.

We can correct this oversight by first letting X_{out} denote the union of the discretization nodes on the contour Γ_{out} and the nodes in $Z\backslash Z_{\text{out}}$ and letting Y_{in} be the union of the discretization nodes on Γ_{in} and the nodes in $Z\backslash Z_{\text{in}}$. Then, we form approximate factorizations

$$\|A(Z_{\text{in}}, X_{\text{in}}) - R\widetilde{A}(Z_{\text{in}}, X_{\text{in}})\| < \epsilon$$

and

$$\|A(X_{\text{out}}, Z_{\text{out}}) - \widetilde{A}(X_{\text{out}}, Z_{\text{out}})L, \|_2 < \epsilon,$$

where $\widetilde{A}(Z_{\text{in}}, X_{\text{in}})$ is obtained by subsampling the rows of $A(Z_{\text{in}},X_{\text{in}})$ and $\widetilde{A}(X_{\text{out}}, Z_{\text{out}})$ is obtained by subsampling the columns of $A(X_{\text{out}},Z_{\text{out}})$. The final scattering matrix is given by

$$L\begin{pmatrix} I & -S_1A(Z_1,Z_2) \\ -S_2A(Z_2,Z_1) & I \end{pmatrix}^{-1} \begin{pmatrix} S_1 & 0 \\ 0 & S_2 \end{pmatrix} R. \tag{3.14}$$

The factorizations performed while combining two scattering matrices can be accelerated through the use of proxies, just as in the preceding section.

3.5. A fast direct solver

A procedure for rapidly constructing scattering matrices for the boundary value problem (1.1) is now clear. First, the discretization nodes $Z_{\partial\Omega}$ on $\partial\Omega$ are divided into N sets $Z_1,\ldots,Z_N$. Next, a scattering matrix is formed for each of the sets $Z_1,\ldots,Z_N$. Those scattering matrices are then recursively combined until a scattering matrix for the entire boundary curve is obtained. In short, a hierarchical decomposition of the discretization nodes on $\partial\Omega$ is the last ingredient needed to build a fast direct solver for the boundary value problems of Section 1.

Naive approaches to the construction of such decompositions usually result in poor performance. See, for instance, Section 4.6 of [22] for a discussion of the difficulties which can arise. For the experiments of this paper, we used a spatial decomposition of the discretization nodes in order to form the necessary hierarchical decomposition. More specifically, we first apply a random rotation to the discretization nodes on $\partial\Omega$ in order to form a set of points $z_1,\ldots,z_n$ which are identified with the original discretization nodes. A standard quadtree data structure for the points $z_1,\ldots,z_n$ is now formed. This is accomplished by recursively dividing a square which bounds the scatterer $\partial\Omega$. In each iteration, a box is divided into 4 equal sized "child" subboxes if it contains more than a user-specified number of points. The quadtree boxes formed in this fashion are then processed in a bottom-up fashion; that is, a box is processed only after each of its child boxes have been processed. Childless boxes are processed by forming a scattering matrix for the discretization nodes associated with the points contained inside of it. Boxes which have children are processed by combining the scattering matrices which are associated with its children. The output of this procedure is a scattering matrix for the boundary value problem.

4. Numerical experiments

This section describes several numerical experiments performed to assess the approach of this paper. They were carried out on a PC equipped with a 2.67 GHz Intel Core i7 processor and 12 GB of RAM. Code for the experiments was written in Fortran 77 and compiled with the Intel Fortran Compiler version 12.0.3 using the flag "-O3." No attempt was made to parallelize the code and no optimized linear algebra libraries were used — that is, the timings given below are those obtained using straightforward Fortran implementations of basic linear algebraic operations such as matrix inversion and matrix multiplication. One of the principal limitations on obtainable accuracy in the experiments that follow is the precision to which Hankel functions are evaluated. We used subroutines for the evaluation of Hankel functions which achieve roughly 13 digits of relative precision. This effectively places a bound on the achievable accuracy of the experiments described here.

In a number of instances in what follows, we refer to bounding circles for planar regions and bounding annuli for planar curves. In our experiments, bounding circles were constructed by sampling a large number of points $(x_1,y_1), (x_2,y_2) \ldots, (x_N,y_N)$ on the boundary of the region, taking the center of the circle to be the point (x_0,y_0) defined by

$$x_0 = \frac{1}{N}\sum_{j=1}^{N} x_j \quad \text{and} \quad y_0 = \frac{1}{N}\sum_{j=1}^{N} y_j,$$

and letting the radius be the maximum of the set

$$\left\{ \sqrt{(x_j - x_0)^2 + (y_j - y_0)^2} : j = 1, \ldots, N \right\}.$$

This is a somewhat crude mechanism which can fail in certain cases (for instance, the center of the bounding circle need not fall inside of the domain under consideration), but it was sufficient for our purposes. Bounding annuli were formed in an analogous fashion.

4.1. Conditioning

In this first collection of experiments, we estimated the condition numbers of several scattering theoretic integral operators given on domains with a small number of corner points. It would be desirable to conduct experiments involving larger-scale domains, but the computation of the singular values of integral operators given on such domains is not computationally feasible using standard algorithms.

We considered the compact domain Ω_{clover} whose boundary is given by the polar equation

$$r(\theta) = \frac{1}{2} + |\cos(2\theta)|, \quad -\pi < \theta < \pi,$$

and the polygonal domain Ω_{triangle} with vertices $(-5/4, -3/4)$, $(3/4, -3/4)$ and $(3/4,5/4)$. Fig. 2 depicts the domains Ω_{clover} and Ω_{triangle}. Each experiment consisted of forming a discretization of the integral operator associated with an exterior Neumann or exterior Dirichlet problem given on one of the these domains using the algorithm of Section 2, computing the condition number of that discretization and solving an instance of the boundary value problem. Note that standard Nyström

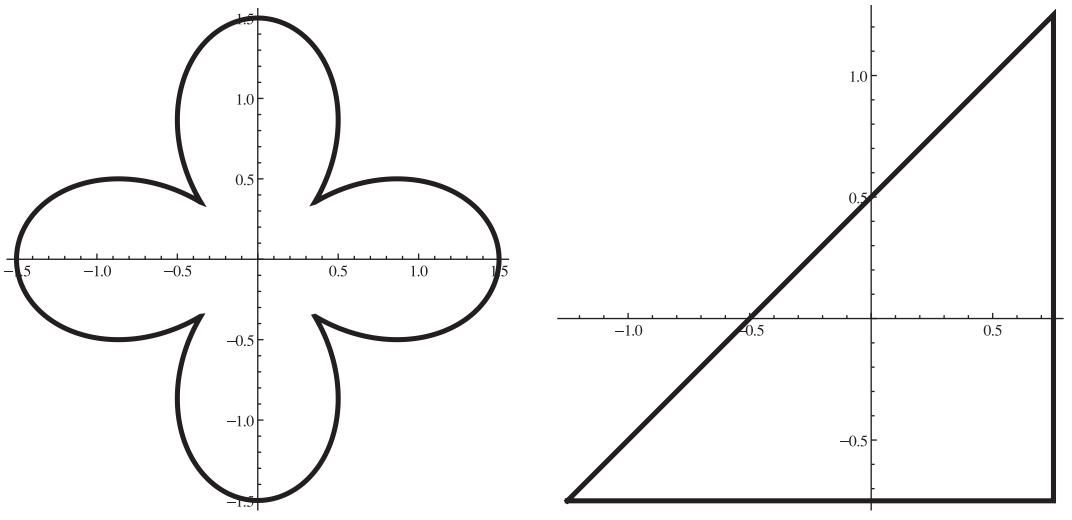

Fig. 2. The domains Ω_{clover} (left) and Ω_{triangle} (right).

Table 2
The L^2 condition numbers of the operators associated with the Neumann and Dirichlet problems on certain Lipschitz domains.

Domain	ω	Dirichlet			Neumann		
		N	κ	E	N	κ	E
Ω_{clover}	2π	1760	$5.01 \times 10^{+1}$	1.10×10^{-13}	5520	$7.22 \times 10^{+1}$	1.33×10^{-13}
	5π	1760	$5.29 \times 10^{+1}$	2.48×10^{-13}	5730	$4.22 \times 10^{+2}$	7.33×10^{-13}
	10π	2240	$6.99 \times 10^{+1}$	8.16×10^{-13}	6330	$5.72 \times 10^{+2}$	2.77×10^{-13}
Ω_{triangle}	2π	2970	$2.75 \times 10^{+1}$	3.15×10^{-13}	1120	$7.56 \times 10^{+1}$	2.99×10^{-14}
	5π	3040	$2.51 \times 10^{+1}$	8.01×10^{-14}	1240	$3.73 \times 10^{+1}$	8.92×10^{-15}
	10π	3320	$2.63 \times 10^{+1}$	2.40×10^{-13}	1520	$3.01 \times 10^{+2}$	7.70×10^{-14}

techniques, when applied to integral operators of this type, generally result in highly ill-conditioned matrices; see, for instance, [6].

In each experiment, the boundary data was taken to be a potential generated by a unit charge distribution on a circle of radius 0.1 centered at the origin; that is,

$$g(x) = \int_{|y|=0.1} H_0(\omega|x-y|)ds(y).$$

The accuracy of the obtained solution was measured by computing the relative $L^2(\Gamma)$ error, where Γ is the circle of radius 5 centered at the origin. Table 2 reports the results of these experiments. There, ω refers to the wavenumber for the problem, κ is the L^2 condition number of the integral operator, and E is the error estimate for the solution. Note that the operator

$$T : L^2(\partial\Omega_{\text{triangle}}) \to L^2(\partial\Omega_{\text{triangle}})$$

defined by

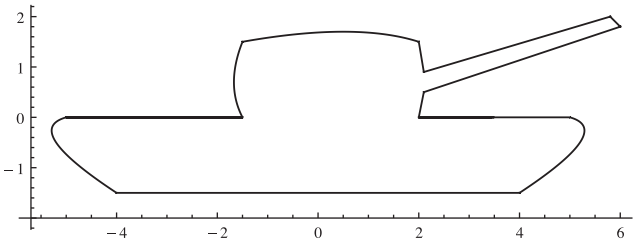

Fig. 3. The domain Ω_{tank}.

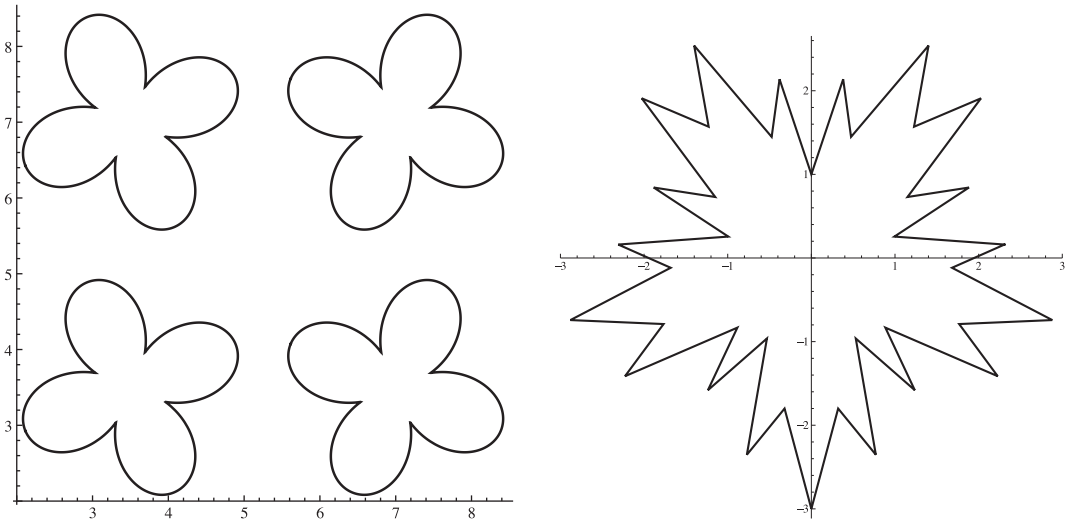

Fig. 4. The domains Ω_{clovers} (left) and Ω_{star} (left).

$$T\sigma(x) = -\frac{1}{2}\sigma(x) + \frac{i}{4}\int_{\Omega_{\text{triangle}}} \omega|x-y|H_1(\omega|x-y|)\frac{(y-x)\cdot\eta_x}{|x-y|^2}\sigma(y)ds(y)$$

has a dimension one nullspace when ω is 5π and when ω is 10π. Nonetheless, as Table 2 shows, the condition numbers of the integral operators arising from the modified formulation of Section 1.2 are quite small.

4.2. Scattering matrices for Neumann and Dirichlet problems

In this next set of experiments, we constructed scattering matrices for exterior Dirichlet and exterior Neumann problems given on the 12 corner "tank" domain Ω_{tank} shown in Fig. 3 as well as the 16 corner "field of clovers" domain Ω_{clovers} and the 38 corner "starburst" domain Ω_{star}, both of which are shown in Fig. 4.

In each experiment, a scattering matrix for either an exterior Neumann or exterior Dirichlet problem given on one of these domains was formed. The contour Γ_{in} was taken to be a union of circles

$$C_1 \cup C_2 \cup \ldots C_N,$$

one for each connected component of the domain. In order to construct the contour C_j, first a bounding annuli A_j for the jth connected component of the domain was formed. Let r_j be the inner radius of A_j and denote by p_j the center point of the annulus A_j. The contour C_j was taken to be the circle of radius $r_j/2$ centered at p_j. The contour Γ_{out} was formed by finding a bounding circle for the entire domain and doubling its radius.

After each scattering matrix was constructed, it was used to solve an instance of the associated boundary value problem and the error in the resulting solution was measured. For Dirichlet problems, the boundary data was taken to be of the form

$$g(x) = \int_{C_{\text{in}}} H_0(\omega|x-y|)ds(y),$$

while for Neumann problems it was of the form

$$g(x) = \int_{C_{\text{in}}} \omega|x-y|H_1(\omega|x-y|)\frac{(y-x)\cdot\eta_x}{|x-y|^2}ds(y).$$

In each case, the contour C_{in} consisted of a union of circles

$$D_1 \cup D_2 \cup \ldots D_N$$

with D_j a circle of radius $r_j/5$ centered at the point $p_j + q_j$, where q_j was a random point drawn from the uniform probability distribution on the square $[0,r_j/5] \times [0,r_j/5]$. Finally, the $L^2(\Gamma_{\text{out}})$ error in the obtained solution was computed. Table 3 presents the results of these experiments. The notation used there is as follows:

- ω is the wavenumber for the problem;
- N is the number of discretization nodes on the boundary curve;
- $N_{\text{out}} \times N_{\text{in}}$ gives the dimensions of the scattering matrix;
- T is the time, in seconds, required to compute the scattering matrix;
- E is the relative $L^2(\Gamma_{\text{out}})$ error in the obtained solution.

Table 3
Results for the numerical experiments of Section 4.2.

Domain	ω	Dirichlet				Neumann			
		N	$N_{\text{out}} \times N_{\text{in}}$	T	E	N	$N_{\text{out}} \times N_{\text{in}}$	T	E
Ω_{tank}	2π	18750	0114×0174	$2.79 \times 10^{+1}$	1.56×10^{-13}	21600	0114×0178	$2.65 \times 10^{+1}$	8.72×10^{-12}
	5π	18750	0250×0307	$3.22 \times 10^{+1}$	2.33×10^{-13}	24420	0288×0312	$3.88 \times 10^{+1}$	1.80×10^{-12}
	10π	20580	0772×0847	$1.16 \times 10^{+2}$	5.12×10^{-13}	24420	0759×0748	$1.43 \times 10^{+2}$	8.53×10^{-12}
	20π	23460	2015×2186	$1.24 \times 10^{+3}$	1.05×10^{-12}	26220	1949×2317	$1.31 \times 10^{+4}$	2.58×10^{-12}
Ω_{clovers}	2π	08640	0106×0304	$7.64 \times 10^{+1}$	4.01×10^{-13}	23040	0106×0356	$1.19 \times 10^{+2}$	8.67×10^{-12}
	5π	09600	0258×0477	$9.24 \times 10^{+1}$	2.66×10^{-13}	24000	0238×0474	$7.03 \times 10^{+2}$	3.96×10^{-12}
	10π	10560	0784×0757	$4.73 \times 10^{+2}$	5.46×10^{-13}	24960	0772×0921	$3.27 \times 10^{+2}$	3.19×10^{-12}
	20π	21120	3237×3674	$5.46 \times 10^{+3}$	8.41×10^{-12}	29760	3420×3989	$6.61 \times 10^{+3}$	4.84×10^{-12}
Ω_{star}	2π	57600	0089×0144	$1.51 \times 10^{+2}$	1.61×10^{-13}	57600	0085×0153	$1.15 \times 10^{+2}$	6.35×10^{-13}
	5π	57600	0167×0232	$1.54 \times 10^{+2}$	1.52×10^{-12}	61440	0182×0249	$1.22 \times 10^{+2}$	1.61×10^{-12}
	10π	57600	0347×0422	$1.73 \times 10^{+2}$	1.52×10^{-12}	61440	0469×0519	$2.04 \times 10^{+2}$	4.48×10^{-12}
	20π	57600	1547×1538	$6.96 \times 10^{+2}$	7.51×10^{-12}	73320	1505×1506	$6.58 \times 10^{+2}$	5.72×10^{-12}

4.3. Scattering matrices for interface problems

We now describe experiments in which scattering matrices for the boundary value problem (1.12) given on the domains Ω_{triangle} and Ω_{tank} were constructed. Recall that Ω_{triangle} appears in Fig. 2 and Ω_{tank} is shown in Fig. 3.

In each experiment, a scattering matrix for the boundary value problem (1.11) was constructed. For interface problems, the spaces of incoming and outgoing potentials are slightly more complicated than for boundary value problems with Neumann and Dirichlet conditions. In order to describe them to the solver, a bounding annulus A was first formed for the domain under consideration. Denote the inner radius of the annulus by r and the outer radius by R. Let C_1 be a circle of radius $4R$ centered at the same point as the annulus A and let C_2 be a circle of radius $r/4$ centered at the same point as the annulus A. The space of incoming potentials consisted of functions of the form

$$\int_{C_1} H_0(\omega_1|x-y|)f_1(y)ds(y) + \int_{C_2} H_0(\omega_2|x-y|)f_2(y)ds(y),$$

where f_1 and f_2 are sufficiently smooth functions. As for outgoing potentials, the solver was instructed to ensure that if σ and τ are charge distributions satisfying (1.12) and the operators D_ω and S_ω are defined as in Section 1.3, then

$$D_{\omega_1}\sigma(x) + S_{\omega_1}\tau(x) \tag{4.1}$$

is accurately evaluated for x on C_2 and

$$D_{\omega_2}\sigma(x) + S_{\omega_2}\tau(x) \tag{4.2}$$

is accurately evaluated for x on C_1. Once the scattering matrix was constructed, it was used to solve an instance of the problem. In each case, the function g was taken to be

$$g(x) = \int_{C_1} H_0(\omega_1|x-y|)ds(y) + \int_{C_2} H_0(\omega_2|x-y|)ds(y).$$

The error in the obtained solutions was measured by comparing the computed values of (4.1) with the potential

$$\int_{C_2} H_0(\omega_1|x-y|)ds(y)$$

on the circle C_1 and the computed values of (4.2) were compared with

$$\int_{C_1} H_0(\omega_2|x-y|)ds(y)$$

on the contour C_2. Table 4 shows the results for these experiments. There, N once again refers to the number of discretization nodes on the boundary of the domain; T is the time in seconds required to compute the scattering matrix; E_{inner} is the relative $L^2(C_2)$ error in the solution; and E_{outer} is the relative $L^2(C_1)$ error in the solution.

4.4. Large-scale experiments

In these experiments, we constructed scattering matrices for the Neumann problem (1.6) on domains of the type show in Fig. 5. Each of the domains consisted of a square grid of replicas of the 38 corner point domain Ω_{star}.

A scattering matrix for each grid was constructed and an instance of the boundary value problem (1.6) was solved using the scattering matrix. The wavenumber was taken to be $\omega = 1$. For these experiments we choose to prioritize speed over accuracy and parameters were set so as to obtain approximately 9 digits of relative accuracy. The contour Γ_{in} was taken to be collection of 5 circles of radius 0.1 place randomly in the interior of the domain. More specifically, five points were chosen by uniformly sampling points in a bounding box containing the boundary curve and discarding any points p which

Table 4
Results for the experiments of Section 6.3.

Domain	ω_1	ω_2	N	Interface			
				$N_{\text{out}} \times N_{\text{in}}$	T	E_{inner}	E_{outer}
Ω_{triangle}	2π	5π	4560	124×095	$1.41 \times 10^{+2}$	6.90×10^{-13}	2.67×10^{-13}
	2π	10π	4980	098×166	$2.07 \times 10^{+2}$	2.75×10^{-12}	4.19×10^{-13}
	5π	2π	4560	095×124	$1.39 \times 10^{+2}$	2.40×10^{-13}	5.75×10^{-13}
	10π	2π	4980	168×098	$2.00 \times 10^{+2}$	5.87×10^{-13}	1.39×10^{-12}
Ω_{tank}	2π	5π	18750	231×159	$5.73 \times 10^{+2}$	1.98×10^{-13}	5.27×10^{-12}
	2π	10π	22500	317×199	$7.33 \times 10^{+2}$	1.33×10^{-13}	4.33×10^{-13}
	5π	2π	18750	159×231	$5.65 \times 10^{+2}$	2.17×10^{-12}	5.61×10^{-13}
	10π	2π	22500	200×317	$7.12 \times 10^{+2}$	4.59×10^{-13}	6.23×10^{-13}

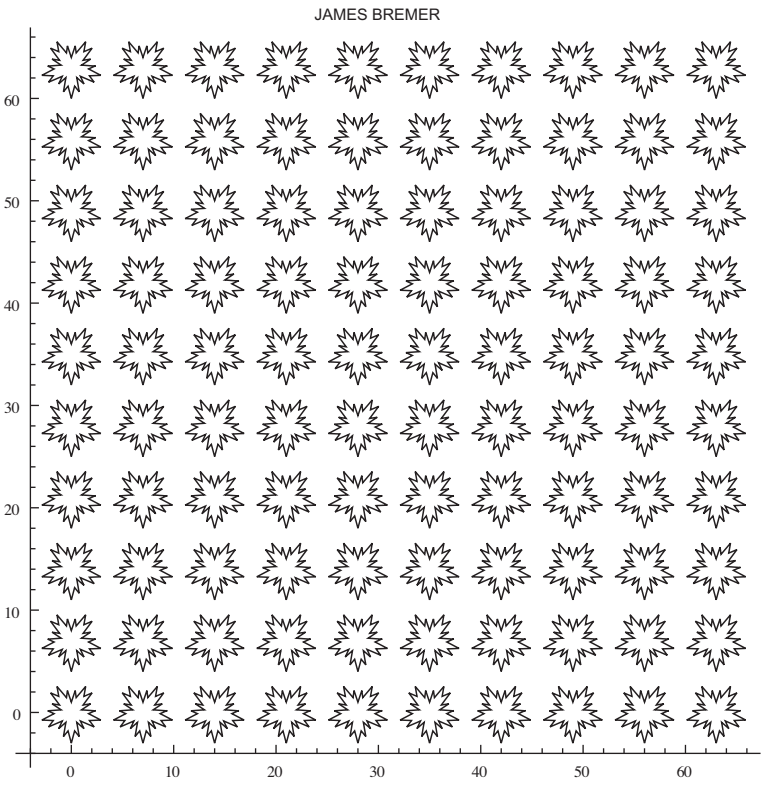

Fig. 5. One of the domains of Section 4.4.

Table 5
Results for the large-scale numerical experiments of Section 6.4.

$N_{\text{stars}} \times N_{\text{stars}}$	N_{corners}	N	$N_{\text{out}} \times N_{\text{in}}$	T	E
1×1	38	21888	59×79	$1.43 \times 10^{+1}$	4.83×10^{-10}
2×2	152	87552	73×94	$6.40 \times 10^{+1}$	3.59×10^{-10}
4×4	608	350208	88×109	$2.59 \times 10^{+2}$	3.28×10^{-10}
8×8	2432	1400832	118×141	$1.06 \times 10^{+3}$	3.67×10^{-10}
10×10	3800	2188800	140×161	$1.63 \times 10^{+3}$	3.38×10^{-10}
16×16	9728	5603328	201×221	$4.40 \times 10^{+3}$	3.46×10^{-10}

were not inside the domain or such that the circle of radius 0.2 centered at p intersected the boundary of the domain. Those five points served as the centers of the circles comprising Γ_{in}. The contour Γ_{out} for outgoing potentials was constructed by finding a bounding circle for the domain and doubling its radius. The incoming potential for each problem was generated by placing a unit charge distribution on each of the circles comprising Γ_{in}. The error in the obtained solution was measured on the circle Γ_{out}.

Note that neither the symmetry of these domains nor their self-similarity was exploited in these experiments. Table 5 shows the results of these experiments; the notation is as follows:

- $N_{\text{stars}} \times N_{\text{stars}}$ gives the dimensions of the grid;
- N_{corners} is the number of corner points on the boundary curve;
- N is the number of discretization nodes on the boundary curve;
- $N_{\text{out}} \times N_{\text{in}}$ gives the dimensions of the scattering matrix;
- T is the time, in seconds, required to compute the scattering matrix;
- E is the relative $L^2(\Gamma_{\text{out}})$ error in the obtained solution.

4.5. Dependence on Γ_{in} and Γ_{out}

In a final set of experiments, we examined the influence of Γ_{in} and Γ_{out} on the size of scattering matrices and the time required to construct them. A collection of scattering matrices for the exterior Dirichlet problem (1.1) given on the domain

Table 6
Results for the numerical experiments of Section 4.5.

R_{in}	R_{out}	$N_{out} \times N_{in}$	T	E	R_{in}	R_{out}	$N_{out} \times N_{in}$	T	E
0.50	2.00	087 × 069	$6.24 \times 10^{+1}$	6.57×10^{-13}	0.50	1.50	125 × 069	$6.18 \times 10^{+1}$	6.78×10^{-13}
0.75	2.00	086 × 115	$6.88 \times 10^{+1}$	6.56×10^{-13}	0.75	1.50	125 × 115	$6.83 \times 10^{+1}$	6.78×10^{-13}
0.90	2.00	084 × 177	$6.55 \times 10^{+1}$	6.57×10^{-13}	0.90	1.50	125 × 177	$6.15 \times 10^{+1}$	6.78×10^{-13}
0.99	2.00	087 × 287	$6.79 \times 10^{+1}$	5.69×10^{-12}	0.99	1.50	125 × 289	$6.58 \times 10^{+1}$	4.41×10^{-12}
0.50	1.10	323 × 069	$7.66 \times 10^{+1}$	7.64×10^{-13}	0.50	1.01	636 × 069	$1.25 \times 10^{+2}$	1.00×10^{-12}
0.75	1.10	323 × 115	$7.14 \times 10^{+1}$	7.63×10^{-13}	0.75	1.01	638 × 116	$1.35 \times 10^{+2}$	1.00×10^{-12}
0.90	1.10	323 × 175	$7.43 \times 10^{+1}$	7.64×10^{-13}	0.90	1.01	638 × 177	$1.25 \times 10^{+2}$	1.00×10^{-12}
0.99	1.10	323 × 289	$7.94 \times 10^{+1}$	6.95×10^{-12}	0.99	1.01	636 × 288	$1.38 \times 10^{+2}$	3.22×10^{-12}

Ω_{clover} shown in Fig. 2 were formed. In each experiment, the wavenumber was taken to be $\omega = 2\pi$ and the contours Γ_{in} and Γ_{out} were circles centered on the origin. The radii of these contours was allowed to vary. All other parameters were fixed. The boundary curve was discretized with 11280 points in all the experiments.

Each scattering matrix was also used to solve instance of the associated boundary value problem. Boundary data was taken to be

$$g(x) = \int_{\Gamma_{in}} H_0(\omega|x-y|)\exp(2iy)ds(y).$$

Here, when we write $\exp(2iy)$, the integration variable y is being treated as a point in the complex plane. The $L^2(\Gamma_{out})$ error in the obtained solution was measured. Table 6 gives the results of these experiments. The notation there is as follows:

- R_{in} gives the radius of the circle Γ_{in} as a multiple of 0.5, which is the distance from the boundary curve $\partial\Omega_{clover}$ to the origin;
- R_{out} is the radius of the circle Γ_{out} as a multiple of 1.5, which is the radius of the smallest circle centered at the origin which encloses the domain Ω_{clover};
- N is the number of discretization nodes on the boundary curve;
- T is the time, in seconds, required to compute the scattering matrix;
- E is the relative $L^2(\Gamma_{out})$ error in the obtained solution.

5. Conclusions

The numerical solution of elliptic boundary value problems on Lipschitz domains has a reputation for difficulty largely because of the delicate constructs which are often used by numerical analysts to address them. The representation of unbounded functions by sampling their values is the principal example. By modifying one of the the standard approaches slightly — we merely replaced sampling of values by sampling of weighted values — robust and analytically sound representations were obtained. This opened the way to applying a simple-minded approach, scattering matrices, and allowed us to solve a class of problems regarded by many as being quite difficult. There is, however, one obvious inefficiency remaining in the approach of this paper. The quadratures being used to discretize corner regions are inefficient. In typical cases, our discretizations require several hundred points per corner. Future work will eliminate this inefficiency by combining variants of the algorithm of [7] for the *numerical* construction of efficient quadrature formulae for corner regions with the fast solver described in this article. This is expected to yield a truly decisive approach to the numerical solution of the integral equations of scattering theory on planar domains with corners.

Acknowledgements

The author is grateful to Vladimir Rokhlin for the benefit of his extensive knowledge of numerical analysis. This work was supported by the Office of Naval Research, under contract N00014–09-1–0318.

References

[1] A. Anand, J. Ovall, C. Turc, Well conditioned boundary integral equations for two-dimensional sound-hard scattering in domains with corners, J. Integral Equ. Appl. (in press).
[2] F. Andriulli, A. Tabacco, G. Vecchi, Solving the EFIE at low frequencies with a conditioning that grows only logarithmically with the number of unknowns, IEEE Trans. Antenn. Propag. 58 (2010) 1614–1624.
[3] A. Björck, Numerical Methods for Least Squares Problems, SIAM, Philadephia, 1996.
[4] J. Bremer, On the Nyström discretization of integral operators on planar domains with corners, Appl. Comput. Harmon. Anal. 32 (2012) 45–64.
[5] J. Bremer, Z. Gimbutas, V. Rokhlin, A nonlinear optimization procedure for generalized Gaussian quadratures, SIAM J. Sci. Comput. 32 (2010) 1761–1788.
[6] J. Bremer, V. Rokhlin, Efficient discretization of Laplace boundary integral equations on polygonal domains, J. Comput. Phys. 229 (2010) 2507–2525.
[7] J. Bremer, V. Rokhlin, I. Sammis, Universal quadratures for boundary integral equations on two-dimensional domains with corners, J. Comput. Phys. 229 (2010) 8259–8280.

[8] O.P. Bruno, J.S. Ovall, C. Turc, A high-order integral algorithm for highly singular PDE solutions in Lipschitz domains, Computing 84 (2009) 149–181.
[9] R. Coifman, Y. Meyer, Wavelets: Calderón-Zygmund and Multilinear Operators, Cambridge University Press, 1997.
[10] D. Colton, R. Kress, Integral Equation Methods in Scattering Theory, John Wiley & Sons, New York, 1983.
[11] D. Colton, R. Kress, Inverse Acoustic and Electromagnetic Scattering Theory, Second ed., Springer-Verlag, New York, 1998.
[12] J. Englund, J. Helsing, Stress computations on perforated polygonal domains, Engrg. Anal. Boundary Elem. 26 (2003) 533–546.
[13] A. Gillman, P. Young, P. Martinsson, A direct solver with $O(n)$ complexity for integral equations on one-dimensional domains. preprint available at <http://arxiv.org/abs/1105.5372>.
[14] M. Gu, S. Eisenstat, Efficient algorithms for computing a strong rank-revealing QR factorization, SIAM J. Sci. Comput. 17 (4) (1996) 848–869.
[15] J. Helsing, The effective conductivity of random checkerboards, J. Comput. Phys. 230 (2011) 1171–1181.
[16] J. Helsing, A fast and stable solver for singular integral equations on piecewise smooth curves, SIAM J. Sci. Comput. 33 (2011) 153–174.
[17] J. Helsing, R. Ojala, Corner singularities for elliptic problems: integral equations, graded meshes, quadrature, and compressed inverse preconditioning, J. Comput. Phys. 227 (2008) 8820–8840.
[18] J. Helsing, R. Ojala, Elastostatic computations on aggregates of grains with sharp interfaces, corners, and triple-junctions, J. Solids Struct. 46 (2009) (pp. 4437–3350).
[19] P. Kolm, S. Jiang, V. Rokhlin, Quadruple and octuple layer potentials in two dimensions I: Analytical apparatus, Appl. Comput. Harmonic Anal. 14 (2003) 47–74.
[20] R. Kress, A Nyström method for boundry integral equations in domains with corners, Numerische Mathematik 58 (1990) 145–161.
[21] R. Kress, Integral Equations, Springer-Verlag, New York, 1999.
[22] P. Martinsson, V. Rokhlin, A fast direct solver for boundary integral equations in two dimensions, J. Comput. Phys. 205 (2006).
[23] P. Martinsson, V. Rokhlin, M. Tygert, On interpolation and integration in finite-dimensional spaces of bounded functions, Commun. Appl. Math. Comput. Sci. 1 (2006) 133–142.
[24] O. Panich, On the question of the solvability of the exterior boundary-value problems for the wave equation and Maxwell's equations, Usp. Mat. Nauk 20A (1965) 221–226.
[25] V. Rokhlin, Solution of acoustic scattering problems by means of second kind integral equations, Wave Motion 5 (1983) 257–272.
[26] V. Rokhlin, Rapid solution of integral equations of scattering theory in two dimensions, J. Comput. Phys. 86 (1990) 414–439.
[27] V. Rokhlin, Diagonal forms of translation operators for the Helmholtz equation in three dimensions, Appl. Comput. Harmonic Anal. 1 (1993) 82–93.
[28] V. Rokhlin, L. Greengard, A fast algorithm for particle simulation, J. Comput. Phys. 73 (1987) 325–348.
[29] F. Woolfe, E. Liberty, V. Rokhlin, M. Tygert, A fast randomized algorithm for the approximation of matrices, Appl. Comput. Harmonics Anal. 25 (2008) 355–366.